An Unconditionally Stable Parallel Splitting Algorithm for the Coupled Stokes-Parabolic Equation Based on the Three-Field Biot Model

Jijing Zhao and Shuyu Sun*[0000−0002−3078−864X]

School of Mathematical Sciences, Tongji University, Shanghai, China
suns@tongji.edu.cn

Abstract. This paper presents a finite element algorithm for solving quasi-static Biot poroelasticity model. By introducing a total pressure, we reformulate the Biot system into a coupled Stokes-parabolic equation. To efficiently solve it, we propose a parallel splitting approach. The coupled system is decomposed into a Stokes subproblem and a parabolic subproblem. These subproblems are then solved in parallel using a stabilization technique. This parallel splitting approach different from sequential or iterative decoupling. The algorithm is proven to be unconditionally stable and theoretical results are validated through numerical experiments.

Keywords: Biot model · Decoupled method · Unconditionally energy stable · Finite element method.

1 Introduction.

This paper addresses the Biot model [3], which has widespread applications in both geological and biological fields. Let $\Omega \times [0,T] \subseteq \mathbb{R}^d, (d=2,3)$ be a bounded polygonal domain with boundary $\partial\Omega$. The classical 2-field formulation of quasi-static poroelasticity model to be studied in this article is given by

$$\begin{aligned} -\nabla\cdot\boldsymbol{\sigma}(\mathbf{u}) + \alpha\nabla p = \mathbf{f} \quad & \text{in } \Omega_T := \Omega\times[0,T], \\ \partial_t(c_0 p + \alpha\nabla\cdot\mathbf{u}) + \nabla\cdot(-\frac{\mathbf{K}}{\mu_f}(\nabla p - \rho_f \mathbf{g})) = q \quad & \text{in } \Omega_T, \end{aligned} \tag{1}$$

where

$$\begin{aligned} \boldsymbol{\sigma}(\mathbf{u}) &= 2\mu\varepsilon(\mathbf{u}) + \lambda\nabla\cdot\mathbf{u}\mathbf{I}, \\ \varepsilon(\mathbf{u}) &= \frac{1}{2}(\nabla\mathbf{u} + (\nabla\mathbf{u})^T). \end{aligned} \tag{2}$$

Here, $\mathbf{u}$ denotes the displacement vector of the solid and p denotes the pressure of the solvent. $\mathbf{f}$ is the body force and $\mathbf{g}$ is the gravitational acceleration, which is assumed to be a constant vector. $\mathbf{I}$ denotes the $d\times d$ identity matrix, and $\varepsilon(\mathbf{u})$ is known as the strain tensor. The parameters in the model are Lamé constants λ and μ; the permeability tensor $\mathbf{K} = \kappa\mathbf{I}$; the solvent viscosity μ_f

ICCS Camera Ready Version 2025
To cite this paper please use the final published version:
DOI: 10.1007/978-3-031-97570-7_23

, Biot–Willis constant α, and the constrained specific storage coefficient c_0. In addition, $\sigma(\mathbf{u})$ is called the (effective) stress tensor. $\hat{\sigma}(\mathbf{u}, p) = \sigma(\mathbf{u}) - \alpha p\mathbf{I}$ is the total stress tensor. $\mathbf{v}_f = -\frac{\mathbf{K}}{\mu_f}(\nabla p - \rho_f \mathbf{g})$ is the volumetric solvent flux.

The Biot model typically involves multiple physical phenomena, and therefore efficient numerical simulation methods for this model have been a focus of research in recent years. As a natural alternative, numerical algorithms that separate fluid mechanics from elasticity have become popular compared to solving large coupled systems. However, the major issue for decoupling methods is instability [7, 9, 10], which is not only related to the time partition scale but also to the material parameters. The main decoupling algorithms for the Biot model are typically categorized into two groups: iterative decoupling algorithms and sequential decoupling methods. Iterative methods, which achieve decoupling by solving submodels iteratively at each time step, still require significant computational time. These iterative algorithms are further divided into four types [9, 10, 8]: drained split, undrained split, fixed strain split, and fixed stress split. Wheeler et al. [12, 11] provided convergence analysis for the undrained and fixed stress methods about two-field Biot model.

The other category is the sequential splitting methods, which decouple the coupled term by using numerical solutions from the previous time step without requiring iteration. These methods allow us to solve the elliptic equation first, followed by the parabolic equation, or vice versa, in a sequential manner. However, they often impose certain constraints on model parameters and time steps. For two-field model, the method of first solving the elliptic equation and then solving the parabolic equation has been proven that the convergence is guaranteed under weak coupling conditions [1, 2]. Some methods enhance stability by adding stabilizers. Riviere et al. [5, 6] originally ensured the stability of the sequential splitting algorithm by adding a small first-order time term and extended this approach to multiphase poroelasticity [14]. Recently, Cai et al. [4] presented an optimal convergence analysis for two sequential methods about three-field Biot model, utilizing a novel proof technique. This three-field model introduces an intermediate variable, known as the total pressure, treating the classical Biot model as a coupling of a generalized Stokes problem and a parabolic problem. However, the aforementioned algorithms all involve sequentially solving subproblems of the Biot model, and the stability of parallel methods for these subproblems has rarely been considered.

In this paper, we propose an unconditionally energy-stable parallel splitting method. Our idea is inspired by [5, 4], but it is worth mentioning that we do not require iterative solving or sequential solving; we can solve the elasticity and parabolic subproblems in parallel. By introducing a total pressure variable, we transform the classical two-field model into a three-field model, specifically a Stokes-parabolic coupled problem. For this coupled equation, we propose a parallel splitting algorithm that enables the parallel computation of the subproblems after decoupling. The Stokes subproblem can be discretized using Taylor-Hood elements that satisfy the inf-sup stability condition, while the parabolic problem can be discretized using Lagrange elements. Furthermore, our proposed time-

ICCS Camera Ready Version 2025
To cite this paper please use the final published version:
DOI: 10.1007/978-3-031-97570-7_23

splitting algorithm can be extended to other discrete methods, including discontinuous Galerkin, weak Galerkin, and virtual element methods. Finally, we provide numerical examples to validate the effectiveness and convergence of the algorithm.

The structure of this paper is as follows. In Section 2, we introduce the mixed formulation of the Biot equation. In Section 3, we present the unconditionally energy-stable splitting parallel scheme. In Section 4, we provide numerical examples to verify the proposed parallel method. Conclusions are drawn in the final Section 5.

2 Modeling equations and energy dissipation law

To close the above system, suitable boundary and initial conditions must be prescribed. The following set of boundary and initial conditions will be considered in this article:

$$
\begin{aligned}
\hat{\boldsymbol{\sigma}}(\mathbf{u},p)\mathbf{n} = \boldsymbol{\sigma}(\mathbf{u})\mathbf{n} - \alpha p\mathbf{n} = \mathbf{f}_1 &\quad \text{on } \Gamma_t := \partial\Omega_t \times [0,T],\\
\mathbf{u} = 0 &\quad \text{on } \Gamma_u := \partial\Omega_u \times [0,T],\\
\mathbf{v}_f \cdot \mathbf{n} = q_1 &\quad \text{on } \Gamma_N := \partial\Omega_N \times [0,T],\\
p = 0 &\quad \text{on } \Gamma_D := \partial\Omega_D \times [0,T].
\end{aligned}
$$

where $\mathbf{n}$ is the unit outward normal to the boundary, $\partial\Omega_t \cup \partial\Omega_u = \partial\Omega$ and $\partial\Omega_N \cup \partial\Omega_D = \partial\Omega$ with $|\Gamma_u| > 0$, $|\Gamma_D| > 0$. Without loss of generality, the above Dirichlet boundary conditions are assumed to be homogeneous. The initial conditions are given by

$$
\mathbf{u} = \mathbf{u}_0, \quad p = p_0 \quad \text{in } \Omega \times \{t = 0\}.
$$

We note that in some engineering literature, the second Lamé constant μ is also called the shear modulus and denoted by G, and $B := \lambda + \frac{2}{3}G$ is called the bulk modulus. λ, μ and B are computed from the Young's modulus E and the Poisson ratio ν by the following formulas:

$$
\lambda = \frac{E\nu}{(1+\nu)(1-2\nu)}, \quad \mu = G = \frac{E}{2(1+\nu)}, \quad B = \frac{E}{3(1-2\nu)}.
$$

We introduce a variable [13],

$$
\xi = \alpha p - \lambda \nabla \cdot \mathbf{u}. \tag{3}
$$

And assume that $\rho_f = 0$ for simplicity. Then problem (1)-(2) can be reformulated as a coupled system of general Stokes equation (or mixed form of the linear elasticity) and parabolic equation,

$$
\begin{aligned}
-\nabla \cdot (2\mu\varepsilon(\mathbf{u})) + \nabla\xi &= \mathbf{f},\\
\nabla \cdot \mathbf{u} + \frac{1}{\lambda}\xi - \frac{\alpha}{\lambda}p &= 0,\\
\left(c_0 + \frac{\alpha^2}{\lambda}\right)\partial_t p - \frac{\alpha}{\lambda}\partial_t\xi + \nabla \cdot (-\mathbf{K}\nabla p) &= q,
\end{aligned} \tag{4}
$$

ICCS Camera Ready Version 2025
To cite this paper please use the final published version:
DOI: 10.1007/978-3-031-97570-7_23

To study the weak form and energy analysis of the 3-field formulation (4), we give the standard sobolev spaces, $W^{m,p}$. $H^m(\Omega)$ for $W^{m,2}(\Omega)$, and $\|\cdot\|_{H^m(\Omega)}$ for $\|\cdot\|_{W^{m,2}(\Omega)}$; $H^m_{0,\Gamma}(\Omega)$ for the subspace of $H^m(\Omega)$ with the vanishing trace on $\Gamma \subset \partial\Omega$. We introduce the following functional spaces: $\mathbf{V} = \{\mathbf{v} \in H^1_{0,\Gamma_u}(\Omega)\}$, $W = L^2(\Omega)$, and $M = \{\phi \in H^1_{0,\Gamma_D}(\Omega)\}$. A 3-tuple $(\mathbf{u}, \xi, p) \in \mathbf{V} \times W \times M$ is called a weak solution to (4), if it holds $\forall t \in [0,T]$,

$$2\mu(\varepsilon(\mathbf{u}), \varepsilon(\mathbf{v})) - (\xi, \nabla\cdot\mathbf{v}) = (\mathbf{f}, \mathbf{v}) + \langle \mathbf{f}_1, \mathbf{v}\rangle, \tag{5}$$

$$(\nabla\cdot\mathbf{u}, \phi) + \frac{1}{\lambda}(\xi, \phi) - \frac{\alpha}{\lambda}(p, \phi) = 0, \tag{6}$$

$$\left(c_0 + \frac{\alpha^2}{\lambda}\right)(\partial_t p, \psi) - \frac{\alpha}{\lambda}(\partial_t \xi, \psi) + (\mathbf{K}\nabla p, \nabla\psi) = (q, \psi) + \langle q_1, \psi\rangle, \tag{7}$$

for $\forall \mathbf{v} \in \mathbf{V}, \forall \phi \in W, \forall \psi \in M$.

Lemma 1. *Every weak solution $(\mathbf{u}, \xi, p)$ of problems (5)-(7) satisfies the following energy law:*

$$\frac{d}{dt}E(t) + (\mathbf{K}\nabla p, \nabla p) = (q, p) + \langle q_1, p\rangle - (\partial_t \mathbf{f}, \mathbf{u}) - \langle \partial_t \mathbf{f}_1, \mathbf{u}\rangle.$$

for $t \in [0,T]$, where $E(t) = \frac{1}{2}\Big[2\mu\|\varepsilon(\mathbf{u}(t))\|^2_{L^2(\Omega)} + \frac{1}{\lambda}\|\alpha p - \xi\|^2_{L^2(\Omega)} + c_0\|p(t)\|^2_{L^2(\Omega)}\Big] - (\mathbf{f}(t), \mathbf{u}(t)) - \langle \mathbf{f}_1(t), \mathbf{u}(t)\rangle$. Moreover, there holds

$$\|\xi\|_{L^2(\Omega)} \le C\left(2\mu\|\varepsilon(\mathbf{u})\|_{L^2(\Omega)} + \|\mathbf{f}\|_{L^2(\Omega)} + \|\mathbf{f}_1\|_{L^2(\Gamma_t)}\right),$$

where C is a positive constant.

3 Unconditionally energy stable parallel splitting method

We define the discrete formulation for a function ϕ at time t_{n+1} as ϕ^{n+1}, where $0 \le n \le N$ and n is integer. The time step size is denoted by $\Delta t = T/N$, $D\phi^{n+1} = \phi^{n+1} - \phi^n$. Additionally, let C represent a generic positive constant that remains independent of mesh and time sizes. Assume $\mathbf{f}_1 = q_1 = 0$ on boundary.

Initial step for $n = 1$, we solve the coupled scheme,

$$2\mu(\varepsilon(\mathbf{u}^1), \varepsilon(\mathbf{v})) - \left(\xi^1, \nabla\cdot\mathbf{v}\right) = (\mathbf{f}^1, \mathbf{v}), \tag{8}$$

$$\left(\nabla\cdot\mathbf{u}^1, \phi\right) + \frac{1}{\lambda}\left(\xi^1, \phi\right) - \frac{\alpha}{\lambda}\left(p^1, \phi\right) = 0, \tag{9}$$

$$\left(c_0 + \frac{\alpha^2}{\lambda}\right)\left(\frac{p^1 - p^0}{\Delta t}, \psi\right) - \frac{\alpha}{\lambda}\left(\frac{\xi^1 - \xi^0}{\Delta t}, \psi\right) + (\mathbf{K}\nabla p^1, \nabla\psi) = (q^1, \psi). \tag{10}$$

For $n \geqslant 2$, the coupling problem is split into subproblems to be computed in parallel,

$$2\mu(\varepsilon(\mathbf{u}^{n+1}), \varepsilon(\mathbf{v})) - \left(\xi^{n+1}, \nabla\cdot\mathbf{v}\right) = (\mathbf{f}^{n+1}, \mathbf{v}), \tag{11}$$

ICCS Camera Ready Version 2025
To cite this paper please use the final published version:
DOI: 10.1007/978-3-031-97570-7_23

$$\left(\nabla\cdot\mathbf{u}^{n+1},\phi\right)+\frac{1}{\lambda}\left(\xi^{n+1},\phi\right)=\frac{\alpha}{\lambda}\left(p^{n},\phi\right), \tag{12}$$

$$\begin{aligned}\left(c_0+\frac{\alpha^2}{\lambda}\right)\left(\frac{p^{n+1}-p^n}{\Delta t},\psi\right)+L\left(\frac{p^{n+1}-2p^n+p^{n-1}}{\Delta t},\psi\right)\\+(\mathbf{K}\nabla p^{n+1},\nabla\psi)=\frac{\alpha}{\lambda}\left(\frac{\xi^n-\xi^{n-1}}{\Delta t},\psi\right)+(q^{n+1},\psi),\end{aligned} \tag{13}$$

for $\forall\mathbf{v}\in\mathbf{V},\forall\phi\in W,\forall\psi\in M$. Next, we prove the energy stability of the proposed parallel time-splitting algorithm.

Theorem 1. *For the initial step $n=1$, (8)-(10) is stable in the sense of*

$$\begin{aligned}&2\mu\|\varepsilon(\mathbf{u}^1)\|^2_{L^2(\Omega)}+\frac{c_0}{2}\|p^1\|^2_{L^2(\Omega)}+\frac{1}{2\lambda}\|\alpha p^1-\xi^1\|^2_{L^2(\Omega)}+\frac{\Delta t\kappa}{2}\|\nabla p^1\|^2_{L^2(\Omega)}\\&\leqslant\mathcal{I}(\mathbf{f}^1,q^1)+\mathcal{I}(\mathbf{u}^0,p^0,\xi^0),\end{aligned} \tag{14}$$

where $\mathcal{I}(\mathbf{f}^1,q^1)=\frac{C_{PF}C_K}{4\mu}\|\mathbf{f}^1\|^2_{L^2(\Omega)}+\frac{\Delta tC_{PF}}{2\kappa}\|q^1\|^2_{L^2(\Omega)}$ is the contribution of the right sourse term, $\mathcal{I}(\mathbf{u}^0,p^0,\xi^0)=2\mu\|\varepsilon(\mathbf{u}^0)\|^2_{L^2(\Omega)}+\frac{c_0}{2}\|p^0\|^2_{L^2(\Omega)}+\frac{1}{2\lambda}\|\alpha p^0-\xi^0\|^2_{L^2(\Omega)}$ is the contribution from the initial time t_0 about displacement and pressure.

Proof. Choose $\mathbf{v}=\mathbf{u}^1-\mathbf{u}^0$ in (8), and $\psi=\Delta tp^1$ in (10). After subtracting (9) at $t=t_0$, take $\phi=\xi^1$, we have

$$2\mu(\varepsilon(\mathbf{u}^1),\varepsilon(\mathbf{u}^1-\mathbf{u}^0))-\left(\xi^1,\nabla\cdot(\mathbf{u}^1-\mathbf{u}^0)\right)=(\mathbf{f}^1,\mathbf{u}^1-\mathbf{u}^0),$$

$$\left(\nabla\cdot\left(\mathbf{u}^1-\mathbf{u}^0\right),\xi^1\right)+\frac{1}{\lambda}\left(\left(\xi^1-\xi^0\right),\xi^1\right)-\frac{\alpha}{\lambda}\left(p^1-p^0,\xi^1\right)=0,$$

$$\left(c_0+\frac{\alpha^2}{\lambda}\right)\left(p^1-p^0,p^1\right)-\frac{\alpha}{\lambda}\left(\xi^1-\xi^0,p^1\right)+\Delta t\kappa(\nabla p^1,\nabla p^1)=(q^1,\Delta tp^1).$$

Summing above equations up, and by Poincaré inequality and Korn inequality, we can obtain (14). □

For the convenience of writing, we define $D_\phi^{n+1}=\phi^{n+1}-\phi^n$.

Theorem 2. *For subsequent step $n\geqslant 2$, if $L\geqslant\dfrac{\tilde{C}\mu\alpha^2}{\lambda^2}$, where constant $\tilde{C}$ is related to C_{PF} and β_0, from Poincare inequality and inf-sup condition respectively. Then we have the following stability,*

$$\begin{aligned}&\mu\sum_{n=1}^{N}\|\varepsilon(D_{\mathbf{u}}^{n+1})\|^2_{L^2(\Omega)}+c_0\sum_{n=1}^{N}\|D_p^{n+1}\|^2_{L^2(\Omega)}+\frac{1}{2\lambda}\sum_{n=1}^{N}\|\alpha D_p^{n+1}-D_\xi^{n+1}\|^2_{L^2(\Omega)}\\&\leq C\left(\sum_{n=1}^{N}\mathcal{I}(\mathbf{f}^{n+1},q^{n+1})+\mathcal{I}(\mathbf{u}^0,p^0,\xi^0)\right),\end{aligned} \tag{15}$$

where $\mathcal{I}(\mathbf{f}^{n+1},q^{n+1})$ is the contribution of the right sourse term, $\mathcal{I}(\mathbf{u}^0,p^0,\xi^0)$ is the contribution from the initial time t_0.

ICCS Camera Ready Version 2025
To cite this paper please use the final published version:
DOI: 10.1007/978-3-031-97570-7_23

Proof. Take the difference between equations (11) and (12) at the $n+1$ time step and the n time step,

$$2\mu(\varepsilon(D_{\mathbf{u}}^{n+1}),\varepsilon(\mathbf{v}))-\left(D_{\xi}^{n+1},\nabla\cdot\mathbf{v}\right)=(D_{\mathbf{f}}^{n+1},\mathbf{v}),\qquad\forall\mathbf{v}\in\mathbf{V},\tag{16}$$

$$\left(\nabla\cdot D_{\mathbf{u}}^{n+1},\phi\right)+\frac{1}{\lambda}\left(D_{\xi}^{n+1},\phi\right)=\frac{\alpha}{\lambda}\left(D_{p}^{n},\phi\right),\qquad\forall\phi\in W,\tag{17}$$

Equation (13) can be rewritten as

$$\begin{aligned}&\left(c_0+\frac{\alpha^2}{\lambda}\right)\left(\frac{D_p^{n+1}}{\Delta t},\psi\right)+L\left(\frac{D_p^{n+1}-D_p^{n}}{\Delta t},\psi\right)+(\mathbf{K}\nabla p^{n+1},\nabla\psi)\\&=\frac{\alpha}{\lambda}\left(\frac{D_\xi^{n}}{\Delta t},\psi\right)+(q^{n+1},\psi).\end{aligned}\tag{18}$$

Setting $\mathbf{v}=D_{\mathbf{u}}^{n+1}$, $\phi=D_{\xi}^{n+1}$, and $\psi=\Delta tD_{p}^{n+1}$, we have

$$\begin{aligned}2\mu(\varepsilon(D_{\mathbf{u}}^{n+1}),\varepsilon(D_{\mathbf{u}}^{n+1}))-\left(D_{\xi}^{n+1},\nabla\cdot D_{\mathbf{u}}^{n+1}\right)&=(D_{\mathbf{f}}^{n+1},D_{\mathbf{u}}^{n+1}),\\\left(\nabla\cdot D_{\mathbf{u}}^{n+1},D_{\xi}^{n+1}\right)+\frac{1}{\lambda}\left(D_{\xi}^{n+1},D_{\xi}^{n+1}\right)&=\frac{\alpha}{\lambda}\left(D_{p}^{n},D_{\xi}^{n+1}\right),\\\left(c_0+\frac{\alpha^2}{\lambda}\right)\left(D_{p}^{n+1},D_{p}^{n+1}\right)+L\left(D_{p}^{n+1}-D_{p}^{n},D_{p}^{n+1}\right)&+\Delta t(\mathbf{K}\nabla p^{n+1},\nabla D_{p}^{n+1})\\&=\frac{\alpha}{\lambda}\left(D_{\xi}^{n},D_{p}^{n+1}\right)+\Delta t(q^{n+1},D_{p}^{n+1}).\end{aligned}$$

Taking above three equations sum up, we have

$$\begin{aligned}&2\mu\|\varepsilon(D_{\mathbf{u}}^{n+1})\|_{L^2(\Omega)}^2+\frac{1}{\lambda}\left(D_{\xi}^{n+1},D_{\xi}^{n+1}\right)-\frac{\alpha}{\lambda}\left(D_{p}^{n+1},D_{\xi}^{n+1}\right)+c_0\|D_{p}^{n+1}\|_{L^2(\Omega)}^2\\&+\frac{\alpha^2}{\lambda}\left(D_{p}^{n+1},D_{p}^{n+1}\right)+L\left(D_{p}^{n+1}-D_{p}^{n},D_{p}^{n+1}\right)+\Delta t(\mathbf{K}\nabla p^{n+1},\nabla D_{p}^{n+1})\\&=(D_{\mathbf{f}}^{n+1},D_{\mathbf{u}}^{n+1})+\Delta t(q^{n+1},D_{p}^{n+1})+\frac{\alpha}{\lambda}\left(D_{p}^{n},D_{\xi}^{n+1}\right)\\&-\frac{\alpha}{\lambda}\left(D_{p}^{n+1},D_{\xi}^{n+1}\right)+\frac{\alpha}{\lambda}\left(D_{\xi}^{n},D_{p}^{n+1}\right).\end{aligned}\tag{19}$$

Noting that

$$\frac{1}{2\lambda}\|\alpha D_{p}^{n+1}-D_{\xi}^{n+1}\|_{L^2(\Omega)}^2=\frac{\alpha^2}{2\lambda}\|D_{p}^{n+1}\|_{L^2(\Omega)}^2+\frac{1}{2\lambda}\|D_{\xi}^{n+1}\|_{L^2(\Omega)}^2-\frac{\alpha}{\lambda}(D_{p}^{n+1},D_{\xi}^{n+1})\tag{20}$$

Taking (20) in (19), we have

$$\begin{aligned}&2\mu\|\varepsilon(D_{\mathbf{u}}^{n+1})\|_{L^2(\Omega)}^2+\frac{1}{2\lambda}\|D_{\xi}^{n+1}\|_{L^2(\Omega)}^2+c_0\|D_{p}^{n+1}\|_{L^2(\Omega)}^2+\frac{\alpha^2}{2\lambda}\|D_{p}^{n+1}\|_{L^2(\Omega)}^2\\&+\frac{1}{2\lambda}\|\alpha D_{p}^{n+1}-D_{\xi}^{n+1}\|_{L^2(\Omega)}^2+\frac{L}{2}\left(\|D_{p}^{n+1}\|_{L^2(\Omega)}^2-\|D_{p}^{n}\|_{L^2(\Omega)}^2+\|D_{p}^{n+1}-D_{p}^{n}\|_{L^2(\Omega)}^2\right)\\&+\frac{\Delta t\kappa}{2}\left(\|\nabla p^{n+1}\|_{L^2(\Omega)}^2-\|\nabla p^{n}\|_{L^2(\Omega)}^2+\|\nabla D_{p}^{n+1}\|_{L^2(\Omega)}^2\right)\\&=(D_{\mathbf{f}}^{n+1},D_{\mathbf{u}}^{n+1})+\Delta t(q^{n+1},D_{p}^{n+1})-\frac{\alpha}{\lambda}\left(D_{p}^{n+1}-D_{p}^{n},D_{\xi}^{n+1}\right)+\frac{\alpha}{\lambda}\left(D_{\xi}^{n},D_{p}^{n+1}\right).\end{aligned}$$

ICCS Camera Ready Version 2025
To cite this paper please use the final published version:
DOI: 10.1007/978-3-031-97570-7_23

Summing over index n from 1 to N, we obtain

$$
\begin{aligned}
&2\mu\sum_{n=1}^{N}\|\varepsilon(D_{\mathbf{u}}^{n+1})\|_{L^2(\Omega)}^2+\frac{1}{2\lambda}\sum_{n=1}^{N}\|D_{\xi}^{n+1}\|_{L^2(\Omega)}^2+c_0\sum_{n=1}^{N}\|D_{p}^{n+1}\|_{L^2(\Omega)}^2\\
&+\frac{\alpha^2}{2\lambda}\sum_{n=1}^{N}\|D_{p}^{n+1}\|_{L^2(\Omega)}^2+\frac{1}{2\lambda}\sum_{n=1}^{N}\|\alpha D_{p}^{n+1}-D_{\xi}^{n+1}\|_{L^2(\Omega)}^2\\
&+\frac{L}{2}\left(\|D_{p}^{N+1}\|_{L^2(\Omega)}^2-\|D_{p}^{1}\|_{L^2(\Omega)}^2+\sum_{n=1}^{N}\|D_{p}^{n+1}-D_{p}^{n}\|_{L^2(\Omega)}^2\right)\\
&+\frac{\Delta t\kappa}{2}\left(\|\nabla p^{N+1}\|_{L^2(\Omega)}^2-\|\nabla p^{1}\|_{L^2(\Omega)}^2+\sum_{n=1}^{N}\|\nabla D_{p}^{n+1}\|_{L^2(\Omega)}^2\right)\\
=&\sum_{n=1}^{N}(D_{\mathbf{f}}^{n+1},D_{\mathbf{u}}^{n+1})+\sum_{n=1}^{N}\Delta t(q^{n+1},D_{p}^{n+1})\\
&-\frac{\alpha}{\lambda}\sum_{n=1}^{N}\left(D_{p}^{n+1}-D_{p}^{n},D_{\xi}^{n+1}\right)+\frac{\alpha}{\lambda}\sum_{n=1}^{N}\left(D_{\xi}^{n},D_{p}^{n+1}\right).
\end{aligned}
\tag{21}
$$

And then we bound the four terms on the right side of (21). Applying the Cauchy-Schwarz inequality, the Young's inequality, the Poincaré inequality and Korn inequality, we have

$$
\sum_{n=1}^{N}(D_{\mathbf{f}}^{n+1},D_{\mathbf{u}}^{n+1})\leqslant\frac{\mu}{2}\sum_{n=1}^{N}\|\varepsilon(D_{\mathbf{u}}^{n+1})\|_{L^2(\Omega)}^2+\frac{C_{PF}C_k}{2\mu}\sum_{n=1}^{N}\|D_{\mathbf{f}}^{n+1}\|_{L^2(\Omega)}^2, \tag{22}
$$

$$
\sum_{n=1}^{N}\Delta t(q^{n+1},D_{p}^{n+1})\leqslant\frac{\Delta t\kappa}{4}\sum_{n=1}^{N}\|\nabla D_{p}^{n+1}\|_{L^2(\Omega)}^2+\frac{\Delta tC_{PF}}{\kappa}\sum_{n=1}^{N}\|q^{n+1}\|_{L^2(\Omega)}^2. \tag{23}
$$

where C_{PF} and C_K are constants from Poincaré inequality and Korn inequality, depending on the domain Ω. Specifically, using the inf-sup condition and (16), we see that the following inequality holds

$$
\begin{aligned}
\beta_0\|D_{\xi}^{n+1}\|_{L^2(\Omega)}&\leqslant\sup_{\mathbf{v}\in\mathbf{V}}\frac{\left|\left(D_{\xi}^{n+1},\nabla\cdot\mathbf{v}\right)\right|}{\|\mathbf{v}\|_{H^1(\Omega)}}\\
&=\sup_{\mathbf{v}\in\mathbf{V}}\frac{\left|2\mu\left(\varepsilon(D_{\mathbf{u}}^{n+1}),\varepsilon(\mathbf{v})\right)+\left(D_{\mathbf{f}}^{n+1},\mathbf{v}\right)\right|}{\|\mathbf{v}\|_{H^1(\Omega)}}\\
&\leqslant 2\mu C\|\varepsilon(D_{\mathbf{u}}^{n+1})\|_{L^2(\Omega)}+C_{PF}\|D_{\mathbf{f}}^{n+1}\|_{L^2(\Omega)},
\end{aligned}
$$

which means that

$$
\|D_{\xi}^{n+1}\|_{L^2(\Omega)}^2\leqslant\tilde{C}\left(\mu^2\|\varepsilon(D_{\mathbf{u}}^{n+1})\|_{L^2(\Omega)}^2+\|D_{\mathbf{f}}^{n+1}\|_{L^2(\Omega)}^2\right), \tag{24}
$$

ICCS Camera Ready Version 2025
To cite this paper please use the final published version:
DOI: 10.1007/978-3-031-97570-7_23

where constant $\tilde{C}$ related to β_0 and C_{PF}. For the third term, by Young inequality, we have

$$\left|\frac{\alpha}{\lambda}\sum_{n=1}^{N}\left(D_p^{n+1}-D_p^n, D_\xi^{n+1}\right)\right| \leqslant \frac{\alpha}{\lambda}\sum_{n=1}^{N}\left(\frac{\delta\|D_p^{n+1}-D_p^n\|^2_{L^2(\Omega)}}{2}+\frac{\|D_\xi^{n+1}\|^2_{L^2(\Omega)}}{2\delta}\right).$$

From (24) and taking $\delta=\frac{\tilde{C}\mu\alpha}{\lambda}$, we have

$$\begin{aligned}\left|\frac{\alpha}{\lambda}\sum_{n=1}^{N}\left(D_p^{n+1}-D_p^n, D_\xi^{n+1}\right)\right| \leqslant & \frac{\tilde{C}\mu\alpha^2}{2\lambda^2}\sum_{n=1}^{N}\|D_p^{n+1}-D_p^n\|^2_{L^2(\Omega)} \\ & +\frac{\mu}{2}\sum_{n=1}^{N}\|\varepsilon(D_{\mathbf{u}}^{n+1})\|^2_{L^2(\Omega)}+C\sum_{n=1}^{N}\|D_{\mathbf{f}}^{n+1}\|^2_{L^2(\Omega)}.\end{aligned} \tag{25}$$

For the last term, we have

$$\left|\frac{\alpha}{\lambda}\sum_{n=1}^{N}\left(D_\xi^n, D_p^{n+1}\right)\right| \leqslant \frac{1}{2\lambda}\sum_{n=1}^{N}\|D_\xi^n\|^2_{L^2(\Omega)}+\frac{\alpha^2}{2\lambda}\sum_{n=1}^{N}\|D_p^{n+1}\|^2_{L^2(\Omega)} \tag{26}$$

Taking (22), (23), (25) and (26) into (21), we have

$$\begin{aligned}&\mu\sum_{n=1}^{N}\|\varepsilon(D_{\mathbf{u}}^{n+1})\|^2_{L^2(\Omega)}+c_0\sum_{n=1}^{N}\|D_p^{n+1}\|^2_{L^2(\Omega)}+\frac{1}{2\lambda}\sum_{n=1}^{N}\|\alpha D_p^{n+1}-D_\xi^{n+1}\|^2_{L^2(\Omega)} \\ &+\frac{L}{2}\|D_p^{N+1}\|^2_{L^2(\Omega)}+\left(\frac{L}{2}-\frac{\tilde{C}\mu\alpha^2}{2\lambda^2}\right)\sum_{n=1}^{N}\|D_p^{n+1}-D_p^n\|^2_{L^2(\Omega)} \\ &+\frac{\Delta t\kappa}{2}\|\nabla p^{N+1}\|^2_{L^2(\Omega)}+\frac{\Delta t\kappa}{4}\left(\sum_{n=1}^{N}\|\nabla D_p^{n+1}\|^2_{L^2(\Omega)}\right) \\ \leqslant & C\sum_{n=1}^{N}\|D_{\mathbf{f}}^{n+1}\|^2_{L^2(\Omega)}+\frac{\Delta t C_{PF}}{\kappa}\sum_{n=1}^{N}\|q^{n+1}\|^2_{L^2(\Omega)}+\frac{1}{2\lambda}\|D_\xi^1\|^2_{L^2(\Omega)} \\ &+\frac{L}{2}\|D_p^1\|^2_{L^2(\Omega)}+\frac{\Delta t\kappa}{2}\|\nabla p^1\|^2_{L^2(\Omega)}\end{aligned}$$

Thus, if $L\geqslant\frac{\tilde{C}\mu\alpha^2}{\lambda^2}$, we have

$$\begin{aligned}&\mu\sum_{n=1}^{N}\|\varepsilon(D_{\mathbf{u}}^{n+1})\|^2_{L^2(\Omega)}+c_0\sum_{n=1}^{N}\|D_p^{n+1}\|^2_{L^2(\Omega)}+\frac{1}{2\lambda}\sum_{n=1}^{N}\|\alpha D_p^{n+1}-D_\xi^{n+1}\|^2_{L^2(\Omega)} \\ \leqslant & C\sum_{n=1}^{N}\|D_{\mathbf{f}}^{n+1}\|^2_{L^2(\Omega)}+\frac{\Delta t C_{PF}}{\kappa}\sum_{n=1}^{N}\|q^{n+1}\|^2_{L^2(\Omega)}+\mathcal{I}_{first} \\ = & \sum_{n=1}^{N}\mathcal{I}(\mathbf{f}^{n+1},q^{n+1})+\mathcal{I}_{first}.\end{aligned}$$

ICCS Camera Ready Version 2025
To cite this paper please use the final published version:
DOI: 10.1007/978-3-031-97570-7_23

where $\mathcal{I}_{first} = \frac{1}{2\lambda}\|D_\xi^1\|^2_{L^2(\Omega)} + \frac{L}{2}\|D_p^1\|^2_{L^2(\Omega)} + \frac{\Delta t\kappa}{2}\|\nabla p^1\|^2_{L^2(\Omega)}$ denotes the contribution of the first time step. From Theorem 1, we have

$$\mathcal{I}_{first} \leqslant C\left(\mathcal{I}(\mathbf{f}^1, q^1) + \mathcal{I}(\mathbf{u}^0, p^0, \xi^0)\right).$$

□

Theorem 3. *Under the same assumptions as in the Theorem 2, we obtain the unconditionally stable energy inequality,*

$$\begin{aligned}
&\frac{\mu}{2}\|\varepsilon(\mathbf{u}^{N+1})\|^2_{L^2(\Omega)} + \left(\frac{c_0}{2} + \frac{L}{2}\right)\|p^{N+1}\|^2_{L^2(\Omega)} + \frac{1}{4\lambda}\|\alpha p^{N+1} - \xi^{N+1}\|^2_{L^2(\Omega)} \\
&+ \frac{\kappa\Delta t}{2}\sum_{n=1}^{N}\|\nabla p^{n+1}\|^2_{L^2(\Omega)} \leqslant C\left(\sum_{n=1}^{N}\mathcal{I}(\mathbf{f}^{n+1}, q^{n+1}) + \mathcal{I}(\mathbf{u}^0, p^0, \xi^0)\right),
\end{aligned} \tag{27}$$

where $\mathcal{I}(\mathbf{f}^{n+1}, q^{n+1})$ is the contribution of the right sourse term, $\mathcal{I}(\mathbf{u}^0, p^0, \xi^0)$ is the contribution from the initial time t_0.

Proof. Setting $\mathbf{v} = D_{\mathbf{u}}^{n+1}$ in (11), making difference from $n+1$ to n for (12) and taking $\phi = \xi^{n+1}$, taking $\psi = \Delta t p^{n+1}$ in (13). Then summing three equations up, we have

$$\begin{aligned}
&\mu\left(\|\varepsilon(\mathbf{u}^{n+1})\|^2_{L^2(\Omega)} - \|\varepsilon(\mathbf{u}^n)\|^2_{L^2(\Omega)} + \|\varepsilon(\mathbf{u}^{n+1} - \mathbf{u}^n)\|^2_{L^2(\Omega)}\right) \\
&+\left(\frac{c_0}{2}+\frac{L}{2}\right)\left(\|p^{n+1}\|^2_{L^2(\Omega)} - \|p^n\|^2_{L^2(\Omega)} + \|p^{n+1} - p^n\|^2_{L^2(\Omega)}\right) + \kappa\Delta t\|\nabla p^{n+1}\|^2_{L^2(\Omega)} \\
&+ \frac{1}{\lambda}\left(\xi^{n+1} - \xi^n, \xi^{n+1}\right) + \frac{\alpha^2}{\lambda}\left(p^{n+1} - p^n, p^{n+1}\right) - \frac{\alpha}{\lambda}\left(p^{n+1} - p^n, \xi^{n+1}\right) \\
&+ \frac{\alpha}{\lambda}\left(p^{n+1} - p^n, \xi^{n+1}\right) - \frac{\alpha}{\lambda}\left(p^n - p^{n-1}, \xi^{n+1}\right) - L(p^n - p^{n-1}, p^{n+1}) \\
&- \frac{\alpha}{\lambda}\left(\xi^{n+1} - \xi^n, p^{n+1}\right) + \frac{\alpha}{\lambda}\left(\xi^{n+1} - \xi^n, p^{n+1}\right) - \frac{\alpha}{\lambda}\left(\xi^n - \xi^{n-1}, p^{n+1}\right) \\
&= \left(\mathbf{f}^{n+1}, D_{\mathbf{u}}^{n+1}\right) + \left(q^{n+1}, \Delta t p^{n+1}\right).
\end{aligned} \tag{28}$$

Noting that

$$\begin{aligned}
&\frac{1}{\lambda}\left(\xi^{n+1} - \xi^n, \xi^{n+1}\right) + \frac{\alpha^2}{\lambda}\left(p^{n+1} - p^n, p^{n+1}\right) \\
&- \frac{\alpha}{\lambda}\left(p^{n+1} - p^n, \xi^{n+1}\right) - \frac{\alpha}{\lambda}\left(\xi^{n+1} - \xi^n, p^{n+1}\right) \\
=&\frac{1}{2\lambda}\left(\|\alpha p^{n+1} - \xi^{n+1}\|^2_{L^2(\Omega)} - \|\alpha p^n - \xi^n\|^2_{L^2(\Omega)}\right. \\
&\left. + \|\alpha p^{n+1} - \xi^{n+1} - (\alpha p^n - \xi^n)\|^2_{L^2(\Omega)}\right).
\end{aligned}$$

Summing over index n from 1 to N for (28), we have

$$\mu\left(\|\varepsilon(\mathbf{u}^{N+1})\|^2_{L^2(\Omega)} - \|\varepsilon(\mathbf{u}^1)\|^2_{L^2(\Omega)} + \sum_{n=1}^{N}\|\varepsilon(\mathbf{u}^{n+1} - \mathbf{u}^n)\|^2_{L^2(\Omega)}\right)$$

ICCS Camera Ready Version 2025
To cite this paper please use the final published version:
DOI: 10.1007/978-3-031-97570-7_23

$$
\begin{aligned}
&+\left(\frac{c_0}{2}+\frac{L}{2}\right)\left(\|p^{N+1}\|^2_{L^2(\Omega)}-\|p^1\|^2_{L^2(\Omega)}+\sum_{n=1}^{N}\|p^{n+1}-p^n\|^2_{L^2(\Omega)}\right)\\
&+\kappa\Delta t\sum_{n=1}^{N}\|\nabla p^{n+1}\|^2_{L^2(\Omega)}+\frac{1}{2\lambda}\left(\|\alpha p^{N+1}-\xi^{N+1}\|^2_{L^2(\Omega)}-\|\alpha p^1-\xi^1\|^2_{L^2(\Omega)}\right.\\
&\left.+\sum_{n=1}^{N}\|\alpha p^{n+1}-\xi^{n+1}-(\alpha p^n-\xi^n)\|^2_{L^2(\Omega)}\right) \qquad (29)\\
=&\sum_{n=1}^{N}\left(\mathbf{f}^{n+1},\mathbf{u}^{n+1}-\mathbf{u}^n\right)+\sum_{n=1}^{N}\left(q^{n+1},\Delta t p^{n+1}\right)-\frac{\alpha}{\lambda}\sum_{n=1}^{N}\left(D_p^{n+1}-D_p^n,\xi^{n+1}\right)\\
&-\frac{\alpha}{\lambda}\sum_{n=1}^{N}\left(D_\xi^{n+1}-D_\xi^n,p^{n+1}\right)+L\sum_{n=1}^{N}(p^n-p^{n-1},p^{n+1})\\
\doteq& T_1+T_2+T_3+T_4+T_5.
\end{aligned}
$$

We bound the terms T_1 and T_2 similar to (22)-(23). For the third term, we have

$$
\begin{aligned}
T_3=&\sum_{n=1}^{N}-\frac{\alpha}{\lambda}\left(D_p^{n+1}-D_p^n,\xi^{n+1}\right) \qquad (30)\\
=&\sum_{n=1}^{N}\left(-\frac{\alpha}{\lambda}\left(D_p^{n+1},\xi^{n+1}\right)+\frac{\alpha}{\lambda}\left(D_p^n,\xi^n\right)+\frac{\alpha}{\lambda}\left(D_p^n,D_\xi^{n+1}\right)\right)\\
=&-\frac{\alpha}{\lambda}\left(D_p^{N+1},\xi^{N+1}\right)+\frac{\alpha}{\lambda}\left(D_p^1,\xi^1\right)+\frac{\alpha}{\lambda}\sum_{n=1}^{N}\left(D_p^n,D_\xi^{n+1}\right)\\
\leqslant&\frac{\alpha^2}{2\lambda\delta}\|D_p^{N+1}\|^2_{L^2(\Omega)}+\frac{\delta}{2\lambda}\|\xi^{N+1}\|^2_{L^2(\Omega)}+\frac{\alpha^2}{2\lambda}\|D_p^1\|^2_{L^2(\Omega)}+\frac{1}{2\lambda}\|\xi^1\|^2_{L^2(\Omega)}\\
&+\sum_{n=1}^{N}\left(\frac{1}{2\lambda}\|D_\xi^{n+1}\|^2_{L^2(\Omega)}+\frac{\alpha^2}{2\lambda}\|D_p^n\|^2_{L^2(\Omega)}\right).
\end{aligned}
$$

Noting that

$$
\|D_\xi^{n+1}\|^2_{L^2(\Omega)}\leqslant\tilde{C}\left(\mu^2\|\varepsilon(D_{\mathbf{u}}^{n+1})\|^2_{L^2(\Omega)}+\|D_{\mathbf{f}}^{n+1}\|^2_{L^2(\Omega)}\right),
$$

Thus, we have

$$
\begin{aligned}
\alpha^2\|D_p^{n+1}\|^2_{L^2(\Omega)}\leqslant&\|\alpha D_p^{n+1}-D_\xi^{n+1}\|^2_{L^2(\Omega)}+\|D_\xi^{n+1}\|^2_{L^2(\Omega)}\\
\leqslant&\|\alpha D_p^{n+1}-D_\xi^{n+1}\|^2_{L^2(\Omega)}+\tilde{C}\left(\mu^2\|\varepsilon(D_{\mathbf{u}}^{n+1})\|^2_{L^2(\Omega)}+\|D_{\mathbf{f}}^{n+1}\|^2_{L^2(\Omega)}\right),
\end{aligned}
$$

Then, by the Theorem 2, we can bound

$$
\sum_{n=1}^{N}\left(\frac{1}{2\lambda}\|D_\xi^{n+1}\|^2_{L^2(\Omega)}+\frac{\alpha^2}{2\lambda}\|D_p^n\|^2_{L^2(\Omega)}\right) \qquad (31)
$$

ICCS Camera Ready Version 2025
To cite this paper please use the final published version:
DOI: 10.1007/978-3-031-97570-7_23

$$\begin{aligned}
&\leqslant \sum_{n=1}^{N} \frac{1}{2\lambda} \|\alpha D_p^n - D_\xi^n\|^2_{L^2(\Omega)} + \sum_{n=1}^{N+1} \frac{C}{\lambda} \left(\mu^2 \|\varepsilon(D_{\mathbf{u}}^n)\|^2_{L^2(\Omega)} + \|D_{\mathbf{f}}^n\|^2_{L^2(\Omega)}\right) \\
&\leqslant C \left(\sum_{n=1}^{N} \mathcal{I}(\mathbf{f}^{n+1}, q^{n+1}) + \mathcal{I}(\mathbf{u}^0, p^0, \xi^0)\right).
\end{aligned}$$

Taking $\delta = \frac{\lambda}{2\tilde{C}\mu}$ in (30), such that

$$\frac{\delta}{2\lambda} \|\xi^{N+1}\|^2_{L^2(\Omega)} \leqslant \frac{\mu}{4} \|\varepsilon(\mathbf{u}^{N+1})\|^2_{L^2(\Omega)} + C\|\mathbf{f}^{N+1}\|^2_{L^2(\Omega)}.$$

Thus by (31), we have

$$\begin{aligned}
T_3 = \sum_{n=1}^{N} -\frac{\alpha}{\lambda} \left(D_p^{n+1} - D_p^n, \xi^{n+1}\right) \leqslant & C \left(\sum_{n=1}^{N} \mathcal{I}(\mathbf{f}^{n+1}, q^{n+1}) + \mathcal{I}(\mathbf{u}^0, p^0, \xi^0)\right) \\
&+ \frac{\mu}{4} \|\varepsilon(\mathbf{u}^{N+1})\|^2_{L^2(\Omega)}.
\end{aligned} \tag{32}$$

Next, we bound the fourth term,

$$\begin{aligned}
T_4 =& \frac{\alpha}{\lambda} \sum_{n=1}^{N} \left(D_\xi^{n+1} - D_\xi^n, p^{n+1}\right) \\
=& \sum_{n=1}^{N} \left(\frac{\alpha}{\lambda} \left(D_\xi^{n+1}, p^{n+1}\right) - \frac{\alpha}{\lambda} \left(D_\xi^n, p^n\right) - \frac{\alpha}{\lambda} \left(D_\xi^n, D_p^{n+1}\right)\right) \\
=& \frac{\alpha}{\lambda} \left(D_\xi^{N+1}, p^{N+1}\right) - \frac{\alpha}{\lambda} \left(D_\xi^1, p^1\right) - \frac{\alpha}{\lambda} \sum_{n=1}^{N} \left(D_\xi^n, D_p^{n+1}\right) \\
\leqslant& \frac{1}{2\lambda^2\delta} \|D_\xi^{N+1}\|^2_{L^2(\Omega)} + \frac{\alpha^2\delta}{2} \|p^{N+1}\|^2_{L^2(\Omega)} + \frac{\alpha^2}{2\lambda} \|D_\xi^1\|_{L^2(\Omega)} + \frac{1}{2\lambda} \|p^1\|^2_{L^2(\Omega)} \\
&+ \sum_{n=1}^{N} \left(\frac{1}{2\lambda} \|D_\xi^n\|^2_{L^2(\Omega)} + \frac{\alpha^2}{2\lambda} \|D_p^{n+1}\|^2_{L^2(\Omega)}\right).
\end{aligned}$$

Noting that

$$\begin{aligned}
\alpha^2 \|p^{n+1}\|^2_{L^2(\Omega)} \leqslant& \|\alpha p^{n+1} - \xi^{n+1}\|^2_{L^2(\Omega)} + \|\xi^{n+1}\|^2_{L^2(\Omega)} \\
\leqslant& \|\alpha p^{n+1} - \xi^{n+1}\|^2_{L^2(\Omega)} + C \left(\mu^2 \|\varepsilon(\mathbf{u}^{n+1})\|^2_{L^2(\Omega)} + \|\mathbf{f}^{n+1}\|^2_{L^2(\Omega)}\right),
\end{aligned}$$

Taking $\delta = \min\{\frac{1}{2\lambda}, \frac{1}{2\tilde{C}\mu}\}$, such that

$$\frac{\alpha^2\delta}{2} \|p^{N+1}\|^2_{L^2} \leqslant \frac{1}{4\lambda} \|\alpha p^{N+1} - \xi^{N+1}\|^2_{L^2(\Omega)} + \frac{\mu}{4} \|\varepsilon(\mathbf{u}^{N+1})\|^2_{L^2(\Omega)} + C\|\mathbf{f}^{N+1}\|^2_{L^2(\Omega)}.$$

ICCS Camera Ready Version 2025
To cite this paper please use the final published version:
DOI: 10.1007/978-3-031-97570-7_23

Therefore, we have

$$\begin{aligned} T_4 =& \frac{\alpha}{\lambda}\sum_{n=1}^{N}\left(D_\xi^{n+1} - D_\xi^{n}, p^{n+1}\right) \\ \leqslant& C\left(\sum_{n=1}^{N}\mathcal{I}(\mathbf{f}^{n+1}, q^{n+1}) + \mathcal{I}(\mathbf{u}^0, p^0, \xi^0)\right) + \frac{\mu}{4}\|\varepsilon(\mathbf{u}^{N+1})\|^2_{L^2(\Omega)} \\ &+ \frac{1}{4\lambda}\|\alpha p^{N+1} - \xi^{N+1}\|^2_{L^2(\Omega)}. \end{aligned} \tag{33}$$

For the last term, we have

$$T_5 = L\sum_{n=1}^{N}(p^n - p^{n-1}, p^{n+1}) \leqslant \sum_{n=1}^{N}\frac{L^2}{\epsilon}\|p^n - p^{n-1}\|^2_{L^2} + \epsilon\|p^{n+1}\|^2_{L^2}. \tag{34}$$

Taking (32), (33), (34) in (29), noting that the term about $\sum_{n=1}^{N}\left\|D_p^n\right\|_{L^2}$ can be controlled by Theorem 2, then we have

$$\begin{aligned} &\frac{\mu}{2}\|\varepsilon(\mathbf{u}^{N+1})\|^2_{L^2(\Omega)} + \left(\frac{c_0}{2} + \frac{L}{2}\right)\|p^{N+1}\|^2_{L^2(\Omega)} + \frac{1}{4\lambda}\|\alpha p^{N+1} - \xi^{N+1}\|^2_{L^2(\Omega)} \\ &+ \frac{\kappa\Delta t}{2}\sum_{n=1}^{N}\|\nabla p^{n+1}\|^2_{L^2} \leqslant C\left(\sum_{n=1}^{N}\mathcal{I}(\mathbf{f}^{n+1}, q^{n+1}) + \mathcal{I}(\mathbf{u}^0, p^0, \xi^0)\right) + \epsilon\sum_{n=1}^{N}\|p^{n+1}\|^2_{L^2(\Omega)}. \end{aligned}$$

Therefore, by discrete Grown's inequality, we can obtain (27). □

4 Numerical test

In this section, we adopt Taylor-Hood elements $(\mathbf{P_2}, P_1)$ for the pair $(\mathbf{u}, \xi)$ and Lagrange finite elements for p, which satisfies the discrete inf-sup condition.

Let the computational domain is $\Omega = [0,1]^2$. We choose the body force $\mathbf{f}$ and the volumetric source/sink term q in (1)-(2) so that the exact solution is as follows,

$$\begin{aligned} &\mathbf{u}(x,y,t) = \begin{pmatrix} e^{-t}\left(sin\,(2\pi y)\,(-1 + cos(2\pi x)) + \dfrac{1}{\mu+\lambda}sin(\pi x)sin(\pi y)\right) \\ e^{-t}\left(sin\,(2\pi x)\,(1 - cos(2\pi y)) + \dfrac{1}{\mu+\lambda}sin(\pi x)sin(\pi y)\right) \end{pmatrix}, \\ &p(x,y,t) = e^{-t}sin(\pi x)sin(\pi y). \end{aligned}$$

We will test the spatial convergence rates of the L^2 and energy norms of displacement and pressure at time $T = 0.5$ in this example. We select the parameters as follows: $E = 1$, $\nu = 0.499999999$, $c_0 = 10^{-7}$, $\kappa = 10^{-6}$, $\alpha = 1$, In this case, the Lamé constant λ is 1.6667×10^8 .

The results obtained by our parallel scheme are listed in Tables 1. The results in these tables indicate that the H^1 error rate for displacement $\mathbf{u}_h$ is 2, while the L^2 error rates for ξ_h and pressure p_h are 2, and the H^1 error rate for p_h is 1.

ICCS Camera Ready Version 2025
To cite this paper please use the final published version:
DOI: 10.1007/978-3-031-97570-7_23

Table 1. Numerical results.

h	Δt	$\lVert \boldsymbol{u} - \boldsymbol{u}_h \rVert_{L^2(\Omega)}$	rate	$\lVert p - p_h \rVert_{L^2(\Omega)}$	rate	$\lVert \xi - \xi_h \rVert_{L^2(\Omega)}$	rate
1/4	1/8	3.491e-02		3.714e-01		1.405e-01	
1/8	1/32	4.085e-03	3.10	1.122e-01	1.73	2.623e-02	2.42
1/16	1/128	4.736e-04	3.11	2.996e-02	1.90	6.027e-03	2.12
1/32	1/512	5.739e-05	3.04	7.681e-03	1.96	1.480e-03	2.03
h	Δt	$\lVert \nabla (\boldsymbol{u} - \boldsymbol{u}_h) \rVert_{L^2(\Omega)}$	rate	$\lVert \nabla (p - p_h) \rVert_{L^2(\Omega)}$	rate	$\lVert \nabla (\xi - \xi_h) \rVert_{L^2(\Omega)}$	rate
1/4	1/8	8.721e-01		2.227e+00		3.532e+00	
1/8	1/32	2.381e-01	1.87	6.725e-01	1.73	1.585e+00	1.16
1/16	1/128	6.120e-02	1.96	2.099e-01	1.68	7.754e-01	1.03
1/32	1/512	1.542e-02	1.99	7.817e-02	1.43	3.857e-01	1.01

4.1 Barry-Mercer's problem

A well-known benchmark problem is the Barry–Mercer problem, which considers a time-dependent fluid injection and production, and for which an analytical series solution is available. We assume that the domain is $\Omega = [0,1]^2$. We assume that the initial values of displacement and pressure are $\mathbf{u} = 0$ and $p = 0$. For details on the boundary condition settings, refer to Figure 1.

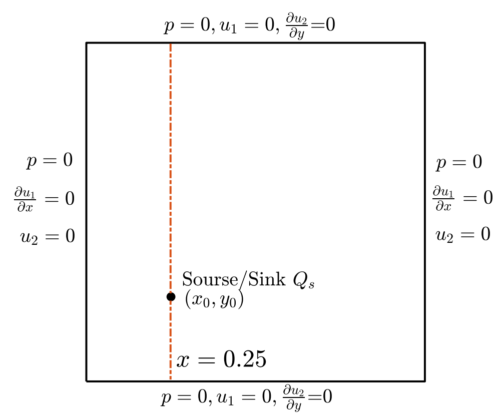

Fig. 1. Rectangle with point x_0 at (0.25, 0.25).

The body force term $\mathbf{f} = \mathbf{0}$, and the source/sink term at source location $(x_0, y_0) = (0.25, 0.25)$ is $Q_s = 2\beta\delta\,(x - x_0)\,\delta\,(y - y_0)\sin(\beta t)$, where $\delta(\cdot)$ denotes the Dirac delta function and $\beta = (\lambda + 2\mu)\kappa$. The physical parameters are given as: $c_0 = 0, \quad \alpha = 1.0, \quad E = 10^5, \quad v = 0.1, \quad \kappa = 10^{-6}$. We will compare our numerical solution with the reference solution. The final time for the solution is $T = \pi/(2\beta)$. The time step size is set to $\Delta t = \pi/(200\beta)$, and the spatial scale is $h = \frac{1}{100}$. Figure 2 illustrates the pressure and displacement distributions for both the analytical and numerical solutions.

ICCS Camera Ready Version 2025
To cite this paper please use the final published version:
DOI: 10.1007/978-3-031-97570-7_23

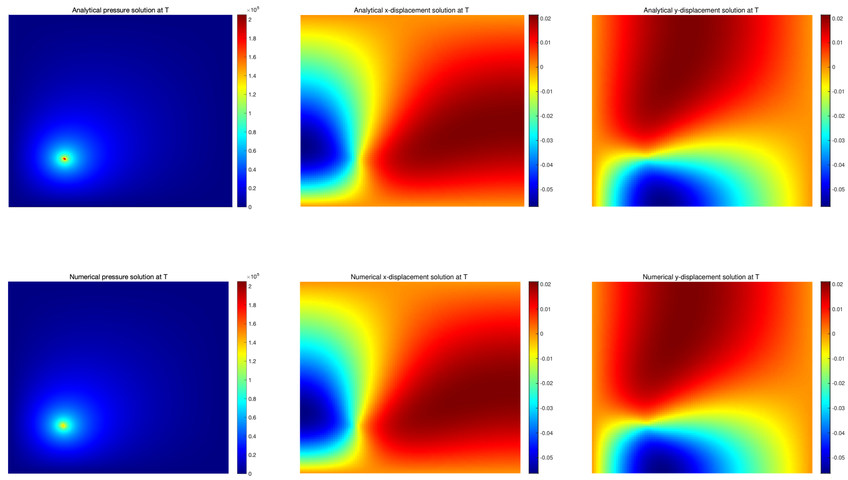

Fig. 2. Distribution about analytic solution (first row) and the numerical solution (second row) at time T. The first column entry is the pressure, the second is the displacement in the x direction, and the third is the displacement in the y direction.

5 Conclusions

This paper presents a paralle time-splitting algorithm for solving the quasi-static Biot poroelasticity model. The three-field Biot system is reformulated as a coupled Stokes-parabolic equation. The algorithm decouples the equation into the Stokes and parabolic subproblems, enabling parallel computation. Semi-discrete scheme is proven to be unconditionally stable.

Acknowledgments. This study was funded by National Key Research and Development Project of China (No. 2023YFA1011701). The work of J. Zhao was supported by the China Postdoctoral Science Foundation under Grant Number GZB20240552 and 2024M762396.

Disclosure of Interests. The authors have no competing interests to declare that are relevant to the content of this article.

References

1. Altmann, R., Maier, R., Unger, B.: Semi-explicit discretization schemes for weakly coupled elliptic-parabolic problems. Math. Comp. **90**(329), 1089–1118 (2021)
2. Altmann, R., Maier, R., Unger, B.: Semi-explicit integration of second order for weakly coupled poroelasticity (2023), arXiv:2203.16664 [cs, math]
3. Biot, M.: Theory of elasticity and consolidation for a porous anisotropic solid. J. Appl. Phys. **26**(2), 182–185 (1955)

ICCS Camera Ready Version 2025
To cite this paper please use the final published version:
DOI: 10.1007/978-3-031-97570-7_23

4. Cai, M., Gu, H., Li, J., Mu, M.: Some optimally convergent algorithms for decoupling the computation of biot's model. J. Sci. Comput. **97** (2023)
5. Chaabane, N., Riviere, B.: A sequential discontinuous galerkin method for the coupling of flow and geomechanics. J. Sci. Comput. **74**, 375–395 (2018)
6. Chaabane, N., Rivière, B.: A splitting-based finite element method for the biot poroelasticity system. Comput. Math. Appl. **75**(7), 2328–2337 (2018)
7. Feng, X., Ge, Z., Li, Y.: Analysis of a multiphysics finite element method for a poroelasticity model. IMA J. Numer. Anal. **38**(1), 330–359 (2018)
8. Gu, H., Cai, M., Li, J.: An iterative decoupled algorithm with unconditional stability for biot model. Math. Comp. **92**(341), 1087–1108 (Jan 2023)
9. Kim, J., Tchelepi, H., Juanes, R.: Stability and convergence of sequential methods for coupled flow and geomechanics: Drained and undrained splits. Comput. Methods Appl. Mech. Eng. **200**(23-24) (2011)
10. Kim, J., Tchelepi, H., Juanes, R.: Stability and convergence of sequential methods for coupled flow and geomechanics: Fixed-stress and fixed-strain splits. Comput. Methods Appl. Mech. Eng. **200**(13-16), 1591–1606 (2011)
11. Mikelić, A., Wang, B., Wheeler, M.F.: Numerical convergence study of iterative coupling for coupled flow and geomechanics. Comput. Geosci. **18**(3-4), 325–341 (Aug 2014)
12. Mikelić, A., Wheeler, M.F.: Convergence of iterative coupling for coupled flow and geomechanics. Comput. Geosci. **17**(3), 455–461 (Jun 2013)
13. Oyarzúa, R., Ruiz-Baier, R.: Locking-free finite element methods for poroelasticity. SIAM J. Numer. Anal. **54**, 5, 2951–2973 (2016)
14. Shen, B., Riviere, B.: A sequential discontinuous galerkin method for two-phase flow in deformable porous media. Comput. Methods Appl. Mech. Eng. **399**, 115266 (2022)

ICCS Camera Ready Version 2025
To cite this paper please use the final published version:
DOI: 10.1007/978-3-031-97570-7_23